Chemistry of Sol–Gel Synthesis of Aluminum Oxides with in Situ Water Formation: Control of the Morphology and Texture

Saloua Rezgui[†] and Bruce C. Gates[*]

Department of Chemical Engineering and Materials Science, University of California, Davis, California 95616

Sandra L. Burkett and Mark E. Davis

Division of Chemistry and Chemical Engineering, California Institute of Technology, Pasadena, California 91125

Received June 29, 1994. Revised Manuscript Received October 3, 1994[⊗]

Sol–gel synthesis of aluminum oxide from mixtures containing $Al(O\text{-}s\text{-}Bu)_3$, acetic acid, and *sec*-butyl alcohol, whereby water was produced in situ, was characterized by infrared, ^{1}H NMR, ^{13}C NMR, and ^{13}C and ^{27}Al magic angle spinning NMR spectroscopies. The molar ratio (R) of acetic acid to $Al(O\text{-}s\text{-}Bu)_3$ strongly influenced the nature of the product. When R was <2, the product was an opaque gelatinous precipitate, and when R was ≥ 2, transparent gels were formed. Acetic acid played crucial roles in both the hydrolysis and condensation reactions that constitute the essential chemistry of the sol–gel synthesis. Acetic acid influenced the rate of hydrolysis by (1) reacting rapidly with $Al(O\text{-}s\text{-}Bu)_3$ to give $Al(O\text{-}s\text{-}Bu_2\text{-}OCOCH_3)$, which is much less reactive than $Al(O\text{-}s\text{-}Bu)_3$ in hydrolysis, (2) catalyzing condensation reactions, and (3) catalyzing the dehydration of *sec*-butyl alcohol to give water. Acetic acid is involved in all the reactions of the sol–gel synthesis and thus provides a delicate control of the chemistry. The ratio R also influenced the morphology of the products formed as a result of drying at temperatures in the range 50–300 °C; these products were characterized by infrared spectroscopy, scanning electron microscopy, and surface area/pore volume measurements. Upon heating, the gelatinous precipitate was transformed into a dense material with a low surface area and low pore volume. Prior to drying, this material contained principally oligomeric species with few OH ligands and little unreacted acetic acid, thus favoring intermolecular condensation reactions and collapse of the structure during drying. In contrast, gels produced at values of $R \geq 2$ gave materials with higher surface areas and higher pore volumes. Prior to drying, these materials contained principally polymeric species incorporating acetate and OH ligands located close to each other, thus favoring intramolecular condensation reactions during drying. Removal of unreacted acetic acid from the gel led to high-surface-area and high-pore-volume materials.

Introduction

Porous transition aluminas are widely used as catalysts[1] and catalyst supports.[2–5] The textural properties are varied over wide ranges by the choice of synthesis conditions,[6–10] but the preparations have been found empirically, and little is understood about the chemistry. The goal of the research summarized here was to understand better the chemistry of the synthesis with $Al(O\text{-}s\text{-}Bu)_3$ in *sec*-butyl alcohol by a sol–gel process, whereby the relative rates of hydrolysis and condensation are controlled by acetic acid. These reactants were chosen because variation of a single parameter, namely, the molar ratio $R = [CH_3COOH]/[Al(O\text{-}s\text{-}Bu)_3]$, allows the synthesis of aluminas with a wide range of textural properties.

The strategy was as follows: (1) The chemistry involved in gel formation and the role of acetic acid were characterized with ^{13}C NMR and ^{27}Al NMR spectroscopy and IR spectroscopy; (2) the steps of dehydration and removal of ligands during drying were characterized with thermal analysis (DTA and TGA), IR, and ^{13}C and ^{27}Al NMR spectroscopies; (3) the texture and morphology of the resultant materials were investigated with measurements of surface area and pore volume and scanning electron microscopy (SEM).

Experimental Methods

Gel Preparations. $Al(O\text{-}s\text{-}Bu)_3$ (98%), s-BuOH (99+%), and glacial acetic acid (99.99%) were supplied by Aldrich. With the reagents in a N_2-filled glovebag (or in air), $Al(O\text{-}s\text{-}Bu)_3$ was

---

[†] Current address: Faculté des Sciences de Bizerte, Zarzouna, Tunisia.

[⊗] Abstract published in *Advance ACS Abstracts,* November 1, 1994.

(1) Sabatier, P.; Reid, E. E. In *Catalysis in organic chemistry*; Van Norstrand: Princeton, NJ, 1922.

(2) Ishiguro, K.; Ishikawa, T.; Kakuta, N.; Ueno, A.; Mitarai, Y.; Kamo, T. *J. Catal.* **1990**, *123*, 523.

(3) Stiles, A. B., Ed. *Catalysts supports and supported catalysts*; Butterworth: Stonehan, 1978.

(4) Dufesne, P.; Payen, E.; Grimblot, J.; Bonnelle, J. P. *J. Phys. Chem.* **1981**, *85*, 2345.

(5) Lopez, T.; Lopez-Gaona, A.; Gomez, R. *J. Non-Cryst. Solids* **1989**, *11*, 170.

(6) Chane-Ching, J. Y.; Klein, L. C. *J. Am. Ceram. Soc.* **1988**, *71*, C 83.

(7) Nazar, L. F.; Klein, L. C. *J. Am. Ceram. Soc.* **1988**, *71*, C 85.

(8) Fanelli, A. J.; Burlew, J. V. *J. Am. Ceram. Soc.* **1986**, *69*, C174.

(9) Armor, J. N.; Carlson, E. J. *J. Mater. Sci.* **1987**, *22*, 2549.

(10) Inoue, M.; Kominami, H.; Inui, T. *J. Am. Ceram. Soc.* **1990**, *73*, 1100.

0897-4756/94/2806-2390$04.50/0

dissolved in stirred *s*-BuOH at room temperature to give a concentration of Al(O-*s*-Bu)$_3$ of 1 M. Various amounts of acetic acid were added to aliquots of this homogeneous solution, yielding gels ($R = [CH_3COOH]/[Al(O\text{-}s\text{-}Bu)_3]$ ranged from 0–4). For $R < 2$, the product was an opaque gelatinous precipitate, and for $R \geq 2$, the products were transparent gels.

Sample Treatment. Each sample of gel or gelatinous precipitate was dried overnight at 70 °C in air and then heated as described below. The drying produced xerogels, but this term is not used below because we wish to distinguish the two classes of samples, namely, those formed from the gelatinous precipitates and those formed from the gels.

Characterization Techniques. *IR Spectroscopy.* The gels were dispersed between two KRS 5 windows and sealed with Parafilm. Spectra of the gels that had been freshly prepared or had been allowed to stand were measured with a Nicolet 510 FTIR spectrometer.

A sample (approximately 20 mg) of each of the dried samples was pressed into a pellet. Spectra were recorded for each gel at temperatures in the range 50–300 °C with N$_2$ flowing over the sample at a rate of 120 mL/min. The purpose of these experiments was to observe changes in the spectra resulting from desorption of organic ligands during the heating. Sample thicknesses decreased as a consequence of the desorption. The spectrometer was a Bruker IFS 66V.

NMR Spectroscopy. ^{13}C NMR spectra of the gels were recorded with a 300-MHz General Electric QE 300 spectrometer. The spectra were recorded with proton decoupling. The samples were placed in 10-mm NMR tubes. The reference compound used in the experiments was TMS (tetramethylsilane). The number of scans recorded for each sample was 240.

^{13}C and ^{27}Al magic angle spinning (MAS) NMR spectra were recorded at the California Institute of Technology with a Bruker AM 300 spectrometer operating at 75.47 MHz for ^{13}C and at 78.21 MHz for ^{27}Al. A 4-μs pulse width with a delay time of 1 s was used for both ^{27}Al and ^{13}C. The gels were packed into 4-mm zirconia rotors and spun at 3 kHz; 3600 and 1800 scans were recorded for ^{13}C and ^{27}Al MAS NMR spectra, respectively. Only freshly prepared samples and gels that had been dried at 180 °C overnight were characterized with this technique. The ^{13}C spectra were recorded with proton decoupling.

Thermal Analysis. Thermogravimetric analysis (TGA) and differential thermal analysis (DTA) curves were obtained simultaneously in static air with a Rigaku PTC-10A instrument. Each sample was placed in a platinum holder and heated from 20 to 800 °C at a rate of 5 °C/min; calcined Al$_2$O$_3$ was used as a reference material.

X-ray Diffraction. Spectra of the dried gels (powders) were measured with a Siemens D 500 diffractometer by using Cu Kα radiation.

SEM. SEM experiments were performed with the gels that had been dried at 70 °C for 24 h and at 180 °C for 24 h. The instrument was an ISI-DS 130 dual-stage scanning electron microscope operating with a filament voltage of 20 keV and a beam current of 100 mA. The gels were deposited onto double-sided tape covering an aluminum specimen stub for mounting of samples; a 300-Å layer of gold film was sputter deposited onto the sample with a BioRad Microscience Division SEM sputter coating system.

Surface Area and Pore Volume Determination. These measurements were made at Chevron Research and Technology Co., Richmond, CA, with a Micromeritics Digisorb instrument with N$_2$ as the adsorbate at −196 °C. The samples were dried and evacuated for an average of 4 h at 300 °C prior to characterization.

Results

Preparation of Gels. When freshly prepared solutions of Al(O-*s*-Bu)$_3$ in *sec*-butyl alcohol were brought in contact with acetic acid, gel formation occurred. The appearance of the gel products depended on the ratio *R*. When *R* was <2, the final product was an opaque gelatinous precipitate. When *R* was ≥2, transparent gels formed. All the products formed within a few minutes at room temperature, and the gel formation was faster for higher values of *R*.

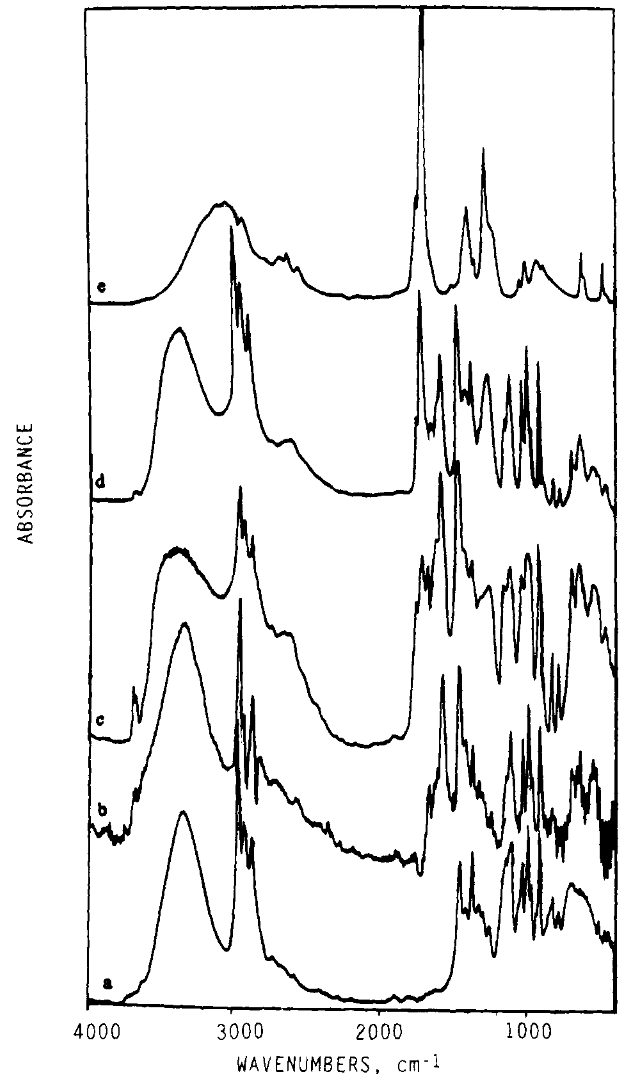

Figure 1. IR spectra of the freshly prepared materials: a, $R = 0$; b, $R = 1$; c, $R = 2$; d, $R = 4$; e, spectrum of neat CH$_3$COOH.

In contrast, when acetic acid wasd added to a solution of Al(O-*s*-Bu)$_3$ that had been allowed to stand for several hours, no gel formation occurred. It has been reported[11] that when the full coordination of the metal is not satisfied in the monomeric metal alkoxide [as is true for Al(O-*s*-Bu)$_3$], the metal atom can increase its coordination number by using vacant d orbitals to accept oxygen from nucleophilic ligands such as OR of another metal alkoxide molecule or of the alcohol solvent, which results in either oligomerization or solvation. Thus it is probable that oligomerization or solvation of the aluminum alkoxide hinders access of acetic acid, thereby preventing gel formation.

IR Spectra of Gels. The IR spectra of the gels before and after aging are shown in Figures 1 and 2. The bands located near 3695 cm^{-1} are attributed to ν_{OH} of basic alumina AlOH species (with no hydrogen bonds).[12]

---

[11] Livage, J.; Henry, M.; Sanchez, C. *Prog. Solid. State Chem.* **1988**, *18*, 259.

[12] Knözinger, H.; Ratnasamy, P. *Catal. Rev. Sci. Eng.* **1978**, *17*, 31.

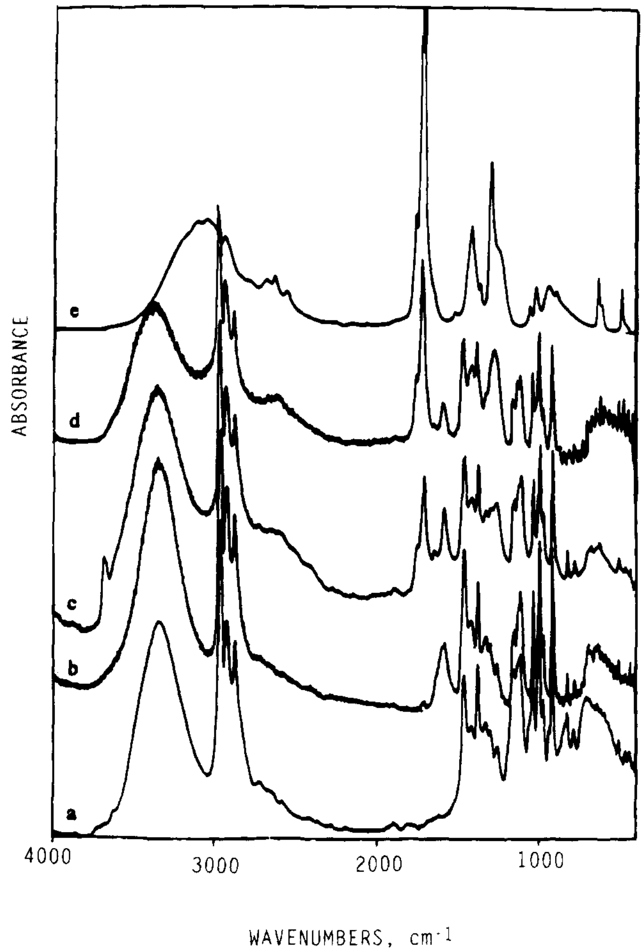

Figure 2. IR spectra of the aged materials: a, $R = 0$; b, $R = 1$; C, $R = 2$; d, $R = 4$; e, spectrum of neat CH_3COOH.

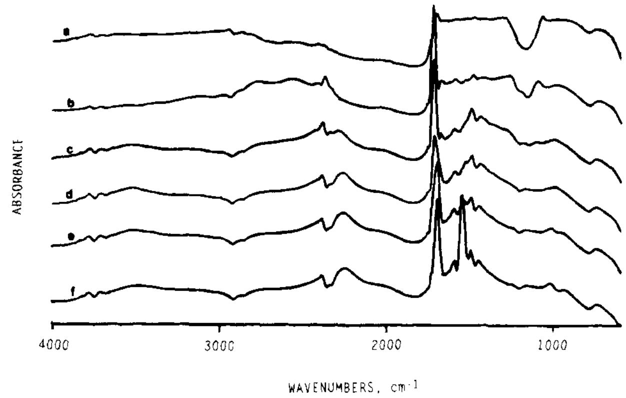

Figure 3. IR spectra of the gelatinous precipitate ($R < 2$) during drying: a, 50 °C; b, 100 °C; c, 200 °C; d, 300 °C; e, after 15 min at 300 °C; f, after 30 min at 300 °C.

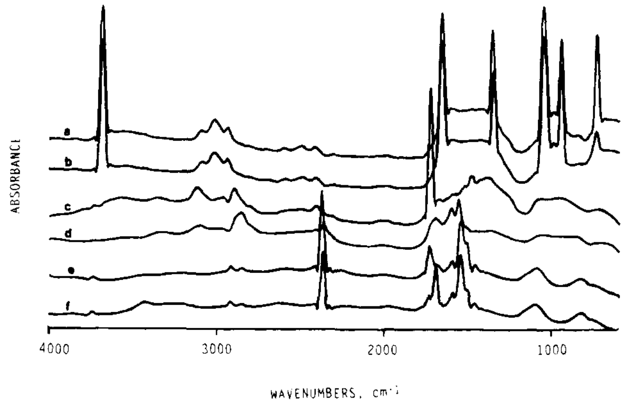

Figure 4. IR spectra of the transparent gels ($R \geq 2$) during drying: a, 50 °C; b, 200 °C; c, 250 °C; d, 280 °C; e, 300 °C; f, after 30 min at 300 °C.

The presence of several bands in this region (Figure 1) indicates that OH groups were present in several different environments. Some of these ν_{OH} bands decreased in intensity or disappeared when the gel aged (Figure 2b–d).

Bands between 1400 and 1800 cm^{-1} are attributed to ν_{COO} of several types of acetate ligands.[13] The relative intensities of these bands changed with R. After the gels had been aged for several hours, only two bands were observed in this region (Figure 2b–d). The band at 1720 cm^{-1} matches that for liquid acetic acid (Figure 2e), and it is attributed to acetic acid in a liquidlike state in the material. By contrast, the ν_{COO} band at 1495 cm^{-1} is thus attributed to bidentate acetate ligands bonded to aluminum.[13,14]

IR Spectra of Dried Gels. The spectra of the gelatinous precipitate (formed when R was <2) are shown as a function of drying temperature in Figure 3. These spectra are characterized by a sharp peak at 1713 cm^{-1}, attributed to ν_{COO} of monodentate acetate ligands,[13,14] which may indicate chemisorbed acetic acid since the frequency is very close to that of liquid acetic acid. As the temperature of the sample reached 300 °C, this peak split into two peaks, at 1700 and 1546 cm^{-1}, which are attributed to C–O stretching vibrations of acetate ligands (the symmetric and the antisymmetric stretching vibrations, respectively). We infer from the splitting of the peaks, $\Delta\nu = 154$ cm^{-1}, that these acetate ligands were bidentate.[13,14]

All of the dried gels had similar spectra, as shown in Figure 4. These spectra include a peak at 3698 cm^{-1} attributed to ν_{OH} and assigned to OH ligands. Generally OH ligands bonded to aluminum appear between 3700 and 3800 cm^{-1}.[12] The lower energy peaks indicate OH groups that are not involved in hydrogen bonding.[12] Several peaks between 3100 and 2880 cm^{-1} are attributed to ν_{CH}. The frequency difference between the peaks at 1654 and 1354 cm^{-1} is characteristic of the symmetric and antisymmetric ν_{COO} of monodentate acetate ligands.[13,14] The peak at 1040 cm^{-1} is attributed to ν_{OH}, and those at 940 and 730 cm^{-1} are attributed to γ_{OH}.

All these peaks decreased in intensity when the drying temperature increased, and were not evident at temperatures >300 °C. At this temperature, the peak indicative of the monodentate acetate ligands transformed into a doublet (at 1690 and 1546 cm^{-1}) attributed to symmetric and antisymmetric COO stretching vibrations, respectively. The value of $\Delta\nu$ (=144 cm^{-1}) implies that these acetate ligands were bidentate.[14] Another peak was observed near 2380 cm^{-1} and is suggested to be related to some carbonyl species.

^{13}C NMR Spectra of Gels. Each of the ^{13}C NMR spectra of Figure 5 includes, in addition to the TMS resonance at 0 ppm, four resonances, at 10, 22, 32, and 69 ppm, attributed to the carbons a–c, respectively, of

---

(13) Nakamoto, N. *Infrared and Raman spectra of inorganic compounds*, 3rd ed.; Wiley: New York, 1978.

(14) Doeuff, S.; Henry, M.; Sanchez, C.; Livage, J. *J. Non-Cryst. Solids* **1987**, *89*, 206.

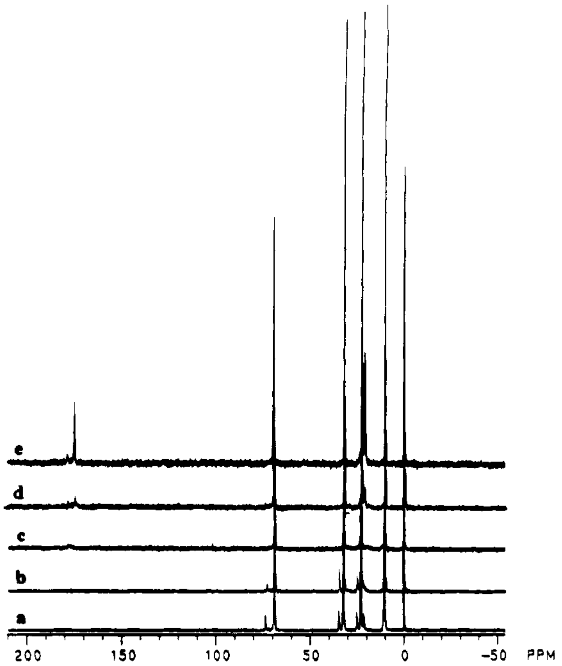

Figure 5. ^{13}C NMR spectra of freshly prepared materials: a, $R = 0$; b, $R = 1$; c, $R = 2$ (spectra for $R = 3$ and $R = 4$ are indistinguishable from that for $R = 2$); d, spectrum of neat CH_3COOH.

the solvent $C_aH_3{-}C_bH_2{-}C_cHOH{-}C_dH_3$. There are four small resonances in two of these spectra (Figure 5a,b) that are similar in position to the resonances attributed to the alcohol. Thus these resonances (observed at 10.5, 25, 35, and 73 ppm) are attributed to the carbons of alkoxide ligands. (The resonance at 21 ppm probably represents an impurity in the metal alkoxide; we suggest that it could be an oligomer containing OR ligands, because it reacted with acetic acid.) As R increased, the resonances at 10.5, 25, 35, and 73 ppm decreased in intensity (Figure 5b). At $R = 2$, new bands appeared at 20, 175, and 179 ppm (Figure 5c). On the basis of a comparison with the spectrum of acetic acid (not shown), the first of these is attributed to CH_3 of acetate ligands. Similarly, the bands at 175 and 179 ppm are attributed to COO species in acetate ligands. The resonance at 175 ppm is in the same position as that of acetic acid itself. That observed at 179 ppm is thus attributed to COO in a different environment; it could be bonded to Al.

^{13}C MAS NMR of Dried Gels. The spectrum (not shown) of each of the samples that had been dried at 180 °C for 24 h (a gelatinous precipitate and the gels) is characterized by only two resonances, at 23 and 179 ppm, which are attributed to the carbons of CH_3 groups and to the carbons of COO groups in acetate ligands bonded to aluminum, respectively.

^{27}Al MAS NMR of Gels. The spectra of a series of products including a gelatinous precipitate and gels are shown in Figure 6. The solution containing $Al(O\text{-}s\text{-}Bu)_3$ as the only aluminum species ($R = 0$) is characterized by a resonance at 4 ppm, which is therefore attributed to the Al atom of $Al(O\text{-}s\text{-}Bu)_3$. As R was increased, resonances appeared at −17, −4.6, and 10.2 ppm. All of these are characteristic of six-coordinate aluminum species.[15–17] Hence they are attributed to aluminum compounds with ligands different from those of the precursor. The species characterized by peaks at −17 and −4.6 ppm were observed for all the R values, but that at 10.2 ppm was observed only for $R = 1$.

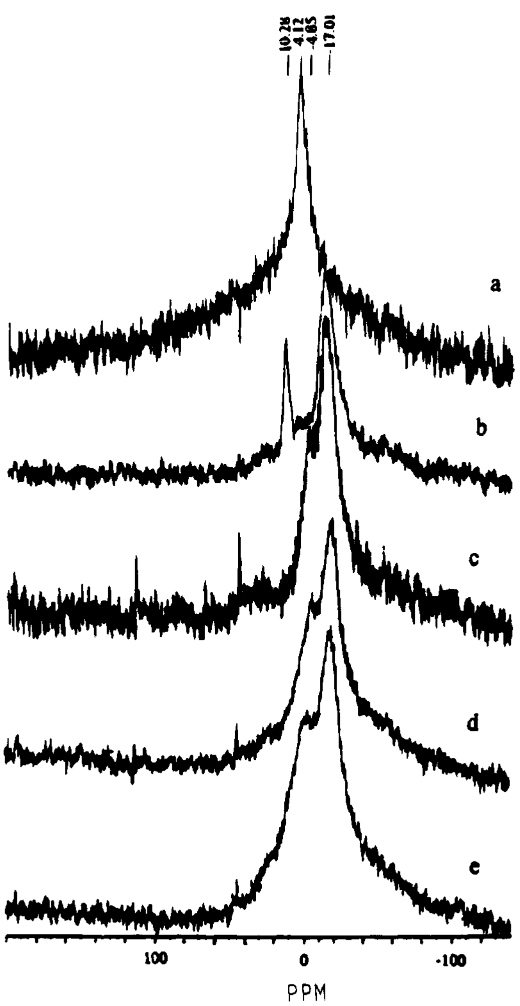

Figure 6. ^{27}Al MAS NMR spectra of freshly prepared materials: a, $R = 0$; b, $R = 1$; c, $R = 2$; d, $R = 3$; e, $R = 4$.

^{27}Al MAS NMR of Dried Gels. The only resonance in each of the spectra (not shown) of each of the samples that had been dried at 180 °C for 24 h was observed at −4 ppm. This is attributed to octahedral six-coordinate aluminum species.[15–17]

X-ray Diffraction. The spectra were broad and featureless, indicating that both the dried gel and the dried gelatinous precipitate were amorphous.

Thermal Analysis. The DTA and TGA curves characterizing the dried gelatinous precipitate and a dried gel are shown in Figure 7. The DTA results show a large endothermic peak starting at room temperature and ending at 180 °C, corresponding to the loss of weakly bonded molecules such as water, alcohol, and acetic acid. A large endothermic peak was observed at about 230 °C, attributed to molecules that had been trapped inside the polymer network. The large exothermic peak between 280 and 440 °C is attributed to combustion of the organic ligands such as O-*s*-Bu and $OCOCH_3$. The loss of mass associated with these

---

(15) Muller, D.; Gessner, W.; Behrends, H. J.; Scheler, G. *Chem. Phys. Lett.* **1981**, *79*, 59.

(16) Fyfe, C. A.; Thomas, J. M.; Klinowski, J.; Gobbi, G. C. *Angew. Chem., Int. Ed. Engl.* **1983**, *22*, 259.

(17) Risbud, S. H.; Kirkpatrick, R. J.; Taglialavore, A. G.; Montez, B. *J. Am. Ceram. Soc.* **1987**, *70*, C10.

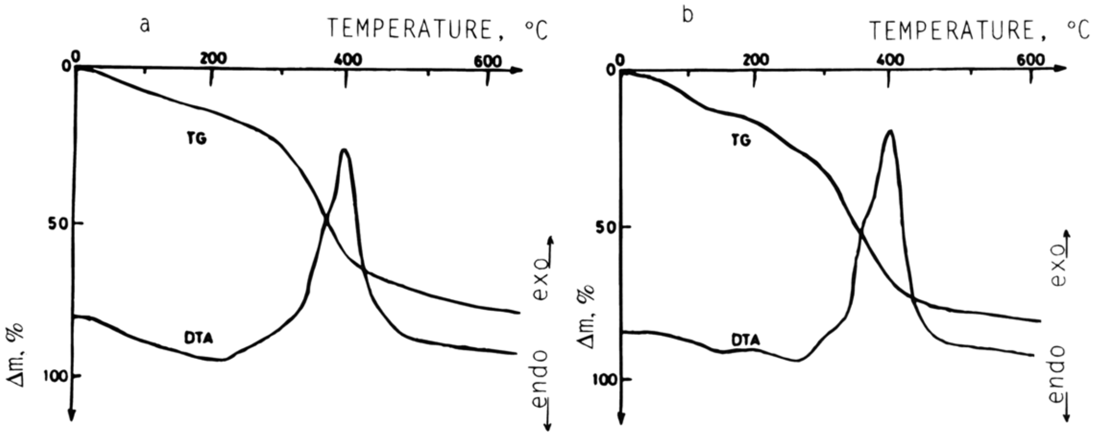

Figure 7. DTA and TG curves for a, $R = 1$; b, $R = 2$.

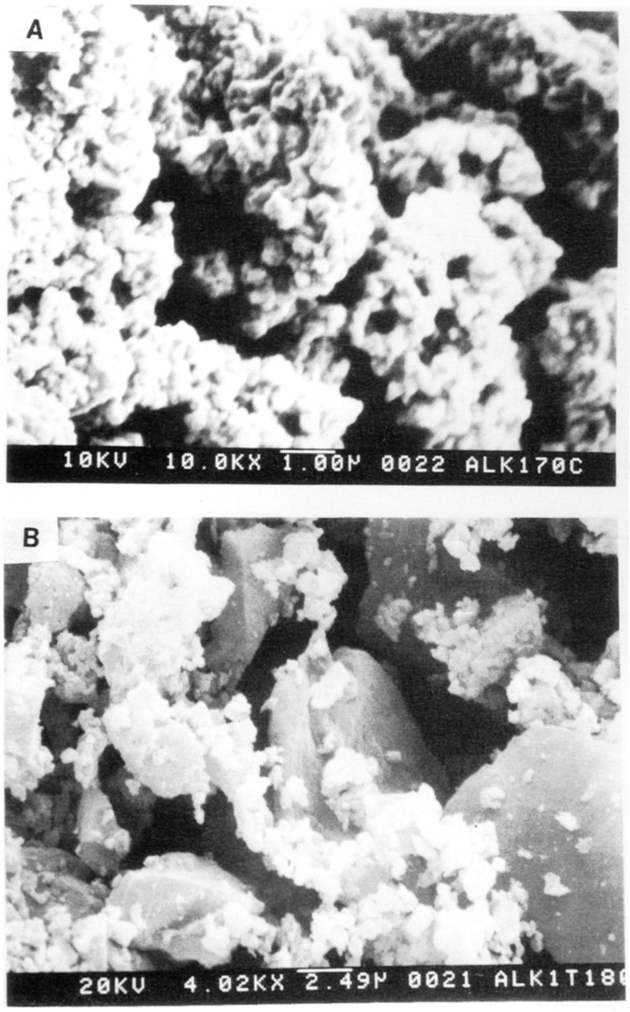

Figure 8. SEM images of the gelatinous precipitate ($R < 2$). A, dried at 70 °C for 24 h; B, dried at 180 °C for 24 h.

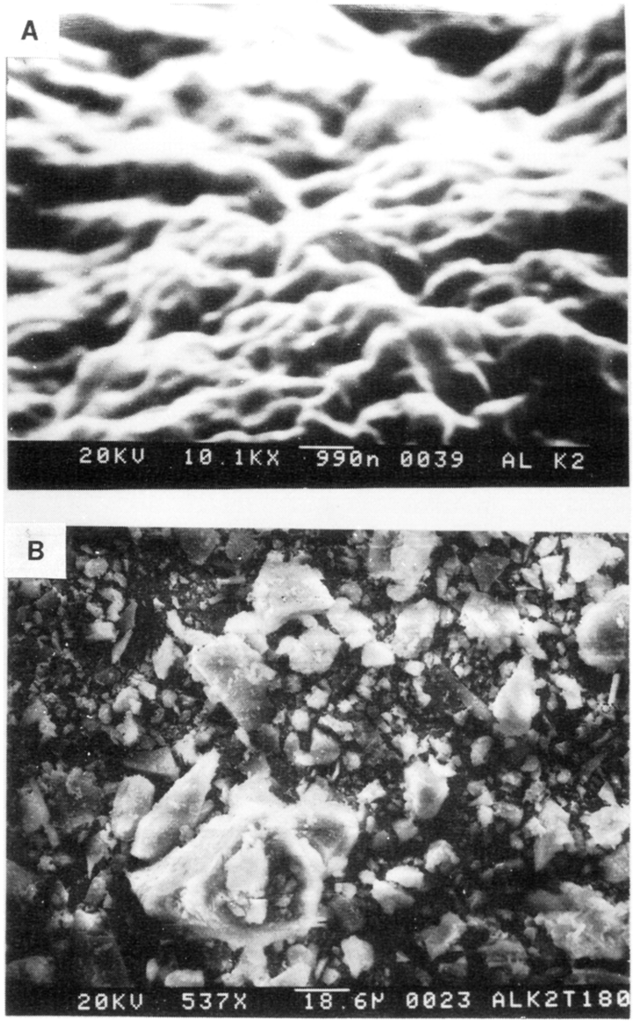

Figure 9. SEM images of the transparent gels ($R \geq 2$). A, dried at 70 °C for 24 h; B, dried at 180 °C for 24 h.

exothermic peaks is the same for the gelatinous precipitate and for the gel (TGA curves, Figure 7).

SEM. Micrographs of the gelatinous precipitates that had been dried at 70 and 180 °C are shown in Figure 8A,B, respectively. Those of the gels dried at 70 and 180 °C are shown in Figure 9A,B, respectively. The gelatinous precipitates (formed when R was <2) dried at 70 °C are porous materials consisting of agglomerated particles (Figure 8A). The gel (formed when R was ≥ 2) dried at 70 °C has a more dense structure with fewer pores than the gelatinous precipitates. The gelatinous precipitates and the gels dried at 180 °C had similar textures (Figures 8B and 9B).

Surface Area/Pore Volume Data. These data are presented in Table 1. The surface area and the total pore volume increased with increasing R.

Discussion

Evidence of Reaction of Acetic Acid with Al(O-*s*-Bu)$_3$. A goal of the research was to understand better the individual reactions involved in gel formation. Evidence of the reactions of acetic acid with the reac-

Table 1. Surface Areas and Pore Volumes of the Different Materials Prepared with Various Amounts of Acetic Acid Represented by the Ratio $R = [CH_3COOH]/[Al(O\text{-}s\text{-}Bu)_3]$

	R			
	1	2	3	4
surface area BET (m^2/g)	14	139	239	253
total pore volume (cm^3/g)	0.02	0.19	0.31	0.29

tants in the sol–gel synthesis is provided by the spectroscopic data.

Modification of the Aluminum Alkoxide Precursor with Acetate Ligands. When acetic acid was first added to a freshly prepared metal alkoxide solution, it reacted rapidly with the metal alkoxide, consistent with eq 1.

$$\begin{aligned}&\text{Al(O-}s\text{-Bu)}_3 + n\text{CH}_3\text{COOH} \rightarrow \\ &\quad \text{Al(O-}s\text{-Bu)}_{3\text{-}n}(\text{CH}_3\text{COO})_n + s\text{-BuOH} \qquad (n \le 3) \quad (1)\end{aligned}$$

Reaction 1 is exothermic, and consistent with its postulated occurrence, we observed a temperature rise as soon as acetic acid was added to the reaction mixture. The IR spectra of aged gels (Figure 2) include, in addition to the ν_{COO} band attributed to unreacted acetic acid, a second ν_{COO} band, at 1495 cm^{-1}, which is the same for all the samples and is attributed to acetate ligands bonded to Al. These ligands have also been observed by ^{13}C MAS NMR of the dried gels. The IR spectra (Figure 2) confirm that acetic acid was still present in the gel for $R \ge 2$ and imply that reaction of acetic acid with $Al(O\text{-}s\text{-}Bu)_3$ did not occur to a large extent and that the product $Al(O\text{-}s\text{-}Bu)_{3\text{-}n}(CH_3COO)_n$ was the same for all values of *R*.

It is known[11,18] that metal alkoxides incorporating acetate ligands are less reactive than the parent metal alkoxides; thus $Al(O\text{-}s\text{-}Bu)_{3\text{-}n}(CH_3COO)_n$ (with $n = 1$) is much less reactive with acetic acid than $Al(O\text{-}s\text{-}Bu)_3$. Mehrotra and Bohra[18] showed that when acetic acid was added to a solution of aluminum isopropoxide, the only product of the reaction was $Al(O\text{-}i\text{-}Pr)_2(CH_3COO)$, and only when the product alcohol was removed continuously could further reaction of $Al(O\text{-}i\text{-}Pr)_2(CH_3COO)$ occur.

Thus, in summary, the data indicate that the reaction of eq 1 took place to give $Al(O\text{-}s\text{-}Bu)_{3\text{-}n}(CH_3COO)_n$ with $n = 1$ but did not proceed further to give products $Al(O\text{-}s\text{-}Bu)_{3\text{-}n}(CH_3COO)_n$ with $n > 1$. Consequently, and in agreement with Mehrotra and Bohra,[18] we infer that steric hindrance essentially prevented the further reaction of $Al(O\text{-}s\text{-}Bu)_2(CH_3COO)$ with acetic acid.

In the case of $R = 1$, the ^{13}C NMR data (Figure 5b) show that $Al(O\text{-}s\text{-}Bu)_3$ was still present in the medium after the reaction to form $Al(O\text{-}s\text{-}Bu)_2(CH_3COO)$ had taken place. The remaining unreacted aluminum alkoxide species were probably oligomeric structures, giving the resonance at 10 ppm in the ^{27}Al MAS NMR spectrum (Figure 6b). This resonance is different from that at 4 ppm characterizing the initial aluminum alkoxide dissolved in *s*-BuOH (Figure 6a). Thus both $Al(O\text{-}s\text{-}Bu)_3$ and $Al(O\text{-}s\text{-}Bu)_2(CH_3COO)$ were present in the gelatinous precipitate formed when $R = 1$. In contrast, when was $R \ge 2$, only the latter species was present.

Evidence of Hydrolysis. The spectroscopic data confirm that water was formed in situ and that it reacted with the aluminum alkoxide species because they indicate that AlOH groups were formed. The IR evidence of these groups is the bands located near 3695 cm^{-1} (Figure 1 and 2), which are attributed to OH ligands that are not hydrogen bonded. These OH ligands can only have been formed from water. Water might have been produced either by esterification (eq 2) or by alcohol dehydration (e.g., eq 3).

$$s\text{-BuOH} + \text{CH}_3\text{COOH} \rightarrow s\text{-BuOCOCH}_3 + \text{H}_2\text{O} \quad (2)$$

$$\text{CH}_3\text{CH}_2\text{-CHOH-CH}_3 \rightarrow \text{CH}_3\text{CH=CHCH}_3 + \text{H}_2\text{O} \quad (3)$$

The first of these reactions, even when it is catalyzed by a mineral acid, is generally slow relative to the reactions of sol–gel synthesis. The second reaction occurs and can be catalyzed by alumina. Léaustic and Riman[19] investigated similar reactions under conditions relevant to sol–gel synthesis, namely, the formation of water from (1) *tert*-butyl alcohol in solutions containing acetic acid and from (2) *tert*-butyl alcohol in solutions containing sulfuric acid. Léaustic and Riman reported that water was produced by alcohol dehydration at 70 °C, but the esterification rate was negligible. We have also tried the same process by using magnesium alkoxide in the absence of aluminum alkoxide, but no gel was observed. This result shows that in the absence of aluminum alkoxide, no water was formed and hence hydrolysis and condensation did not occur. We infer that water formation was catalyzed only in the presence of aluminum alkoxide. Furthermore, when ethanol was used instead of *sec*-butyl alcohol, no gel formation occurred; ethanol dehydration is much slower than *sec*-butyl alcohol dehydration, and thus if water had been formed from ethanol, it would have been by esterification; since gel formation did not occur, we infer that esterification did not occur. The implication is that water formation from *sec*-butyl alcohol took place by catalytic dehydration rather than by esterification.

Water formed in the alcohol dehydration reacts with the metal alkoxides as shown in eqs 4 and 5 (where R is *s*-Bu).

$$\text{Al(O-}s\text{-Bu)}_3 + x\text{H}_2\text{O} \rightarrow \text{Al(O-}s\text{-Bu)}_{3\text{-}x}(\text{OH})_x + x\text{ROH} \quad (4)$$

$$\begin{aligned}&\text{Al(O-}s\text{-Bu)}_2(\text{CH}_3\text{COO}) + x\text{H}_2\text{O} \rightarrow \\ &\quad \text{Al(O-}s\text{-Bu)}_{2\text{-}x}(\text{CH}_3\text{COO})(\text{OH})_x + x\text{ROH} \quad (5)\end{aligned}$$

Condensation Reactions. The products of the hydrolysis reactions are expected to undergo condensation reactions in the presence of acid catalysts:

$$\begin{aligned}&-\text{Al}-\text{O}-s\text{-Bu} + \text{HO}-\text{Al}- \rightarrow \\ &\quad -\text{Al}-\text{O}-\text{Al}- + s\text{-BuOH} \quad (6)\end{aligned}$$

and/or

$$-\text{Al}-\text{OH} + \text{HO}-\text{Al}- \rightarrow -\text{Al}-\text{O}-\text{Al}- + \text{H}_2\text{O} \quad (7)$$

Evidence of the condensation reactions is provided by the IR spectra (Figures 1 and 2) showing that some of the ν_{OH} bands located near 3695 cm^{-1}, attributed to Al–

---

(18) Mehrotra, R. C.; Bohra, R. *Metal Carboxylates*; Academic Press: London, 1978.

(19) Léaustic, A.; Riman, R. E. *J. Non-Cryst. Solids.* **1991**, *135*, 259.

OH species, decreased in intensity or disappeared as the gel aged (Figure 2b–d). When R was ≥ 2, the condensation did not proceed to completion, as shown by the result that Al–OH species were still present (Figure 2d).

The positions of the ^{27}Al MAS NMR resonances observed in the gels for $R \geq 2$ (Figure 6c–e) are inferred to show that Al atoms were present in two separate surroundings. This conclusion is based on comparisons of the NMR spectra with those characterizing numerous materials incorporating condensed aluminum oxide species (e.g., $AlPO_4$'s,[20] clays,[21] and other ceramic materials[22,23]). The band positions show that aluminum was octahedrally coordinated in all the samples.[14–16] The two bands are attributed to Al atoms with OH and OAc ligands. Thus these results confirm that the condensation was not complete. The resonance at −4 ppm is tentatively associated with less highly condensed species (e.g., oligomers), and the resonance at −17 ppm is suggested to be an indication of more highly condensed species (e.g., polymers).

Chemistry of Drying and Morphology of the Dried Materials. In this section we develop an approximate model of the chemistry involved in the drying of the samples. The development is based on the evidence of the ligands in the materials at various stages of the preparation, as indicated by the IR spectra, the thermal analysis, and the texture and morphology of the materials, indicated by the surface area/pore volume and SEM data. Some of the key observations are the differences in ligand composition and morphology of two types of samples, namely, the gels (prepared with $R \geq 2$) and the gelatinous precipitate (prepared with $R < 2$).

Chemistry of Drying. As the samples were dried, DTA curves were measured, showing that the weakly adsorbed species such as water, alcohol, and acetic acid were desorbed at tempeatures <180 °C. The alcohol and acetic acid molecules that were trapped inside the matrix of the polymers as they formed started to desorb from the material at temperatures varying between 200 and 280 °C. Not all of these ligands were observed by IR spectroscopy (Figures 3 and 4), because some had presumably desorbed during the treatment in nitrogen at 50 °C. The remaining organic ligands (O-*s*-Bu and $OCOCH_3$) that were bonded to the solid desorbed from the material at temperatures between 300 and 400 °C.

Both the gel and the gelatinous precipitate incorporated acetate ligands, as shown by ^{13}C MAS NMR. The gels are characterized by OH groups indicated by a sharp band in the IR spectra near 3700 cm^{-1} (Figure 3), and such bands are nearly absent from the spectra characterizing the gelatinous precipitate (Figure 4). The monodentate acetate ligands were evidently transformed during heating into bidentate acetate ligands (Figures 3 and 4). In the gels, this transformation took place at essentially the same temperature, about 300 °C, at which the OH ligands were lost.

The conversion of monodentate acetate ligands into bidentate acetate ligands has been described by Mehrotra and Bohra,[18] who observed that this transformation was accompanied by condensation reactions, as follows:

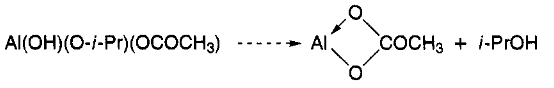

$$\mathrm{Al(OH)(O\text{-}\mathit{i}\text{-}Pr)(OCOCH_3)} \dashrightarrow \mathrm{Al}\underset{O}{\overset{O}{\diamond}}\mathrm{COCH_3} + \mathit{i}\text{-}\mathrm{PrOH}$$

(8)

We postulate that the key to the transformations is the removal of the OH and OR groups, which provide open coordination sites that allow changes in the bonding of the remaining groups, which include both the acetate ligands and the oligomeric and polymeric material. A further postulate is that the removal of the OH and OR groups that is evidenced by the conversion of the monodentate to the bidentate acetate ligands is accompanied by the simultaneous condensation reactions that lead to Al–O–Al bonding and thus to transformation of the structure of the material.

After all the transformations had occurred in both the gelatinous precipitate and the gels, the IR spectra of the various samples (Figures 3 and 4) became almost indistinguishable from each other. This observation implies that the ligation following heat treatment was similar in all of them. Thermal analysis data (Figure 7) also show that both the gelatinous precipitate and the gels are characterized by the same types of curves and the same weight loss at temperatures up to 300 °C. Thus, although the samples were initially different in composition (ligation) and underwent different transformations, in the final states they were similar to each other in their chemical compositions. However, there were significant differences in their morphologies, as discussed in the next section.

Morphology. We propose the following explanation for the morphological differences between these two types of materials (the gelatinous precipitate and the gels) on the basis of their different contents of OH groups and unreacted acetic acid:

The gel that had been (partially) dried at 70 °C (Figure 9A) is characterized by a morphology different from that of the gelatinous precipitate that had been (partially) dried at this same temperature (Figure 8A). The gel, which incorporated a high concentration of OH ligands, as shown by the IR spectra, had a dense but still porous structure. In this case, the protic solvents, such as *s*-BuOH and acetic acid, formed hydrogen bonds with the polymer incorporating Al–OH groups. As the solvent evaporated, the solid network was drawn together to give a dense structure, such as shown in the SEM of Figure 9A. In contrast, the gelatinous precipitate, which incorporated few OH ligands, had a pronounced particulate structure. In this case, only hydrogen bonds with the solvent could form, and thus the molecules were not held together so efficiently after removal of the solvent, and a less dense, particulate structure was formed, as illustrated in the SEM of Figure 8A.

All the samples that had been dried at 180 °C were similar to each other in chemical composition, as described above and indicated by the IR spectra. All these samples were also similar to each other in morphology, as shown by the SEM results of Figures 8B and 9B. However, a stronger basis for comparison of these materials is provided by the surface area/pore volume data, which allow a more detailed interpretation

---

[20] Alemany, L. B.; Timken, H. C.; Johnson, I. D. *J. Magn. Reson.* **1988**, *80*, 427.

[21] Kormaneni, S.; Fyfe, C. A.; Kennedy, G. J.; Strobl, H. *J. Am. Ceram. Soc.* **1986**, *69*, C45.

[22] Kormaneni, S.; Roy, R.; Fyfe, C. A.; Kennedy, G. J.; Strobl, H. *J. Am. Ceram. Soc.* **1986**, *69*, C42.

[23] Bonhomme-Coury, L.; Babonneau, F.; Livage, J. *Chem. Mater.* **1993**, *5*, 323.

of the morphological changes in the materials. The dependence of the surface area on R is similar to the dependence of the pore volume on R (Table 1). As R increased from 1 to 3, the surface area and the pore volume each increased by an order of magnitude, and as R increased from 3 to 4, there was almost no change in either the surface area or the pore volume. As R increased, the amounts of both excess acetic acid (trapped inside the matrix of the polymer network) and Al–OH species increased. The attainment of maxima in the surface area and pore volume when $R = 3$ is suggested to be related to the saturation of the polymer network with unreacted acetic acid at $R = 3$.

A possible explanation to connect the chemistry with the morphological changes is as follows: We envision the formation of dense material as a result of intermolecular condensation reactions whereby reactive groups such as OR and OH groups on neighboring polymer molecules reach each other. These react to form products such as ROH and thereby lead to formation of Al–O–Al bonds linking the neighboring molecules and forming polymeric material that is dense and largely lacking in pores. Such reactions constitute a collapse of the material. In contrast, when the groups that can undergo condensation reactions are close to each other on the same polymer molecule, then the reactions that lead to removal of the ligands can take place by intramolecular reactions, and in this case there will be no collapse of the solid network after the solvent has been removed. Thus the space that was occupied by solvent in the material having a high density of the reactive functional groups will remain as pores after the solvent is removed.

In summary, for $R < 2$, there was no evidence of unreacted acetic acid. As the gelatinous precipitate was dried, the solvent was removed from the network of the polymer, and the remaining material was composed of species having acetate and OR ligands, but with few Al–OH species. As the temperature increased, the reaction of the acetate ligands described in eq 6 could not occur unless OR and OH groups could reach each other, and therefore condensation was intermolecular, leading to a collapse of the polymer into a low-surface-area material.

In contrast, for $R \geq 2$, many OH ligands were present on the polymer in addition to acetate ligands, which made possible the intramolecular condensation between OH, OR, and $OCOCH_3$ ligands that were close to each other, according to eq 6. In this situation the intermolecular condensation reactions were slow in comparison with the intramolecular condensation reactions, and the result was high-area porous materials resulting from the space that had been occupied by the entrapped molecules. When R reached the value of 3, near maxima in surface area and pore volume were attained. If we postulate that the pore volume is determined primarily by the volume of entrapped solvent, then the observations suggest that the gel network became saturated with unreacted acetic acid when R reached the value of 3.

In conclusion, these results show how the use of acetic acid in the synthesis permits the control of the texture of the resultant alumina. The physical and chemical bases of these preparations may be exploited to tailor the pore structure. We can generalize the results as follows: Gelatinous precipitates are transformed into dense materials with low surface areas and low pore volume because they contain principally oligomeric species with many OR ligands and little unreacted acetic acid, thus favoring intramolecular condensation reactions. In contrast, gels give materials with higher surface areas and pores volumes, and the ratio R is crucial in controlling the final structure.

Acknowledgment. S. Rezgui was supported by a Fulbright Fellowship sponsored by AMIDEAST and was on leave from Faculté des Sciences de Bizerte, Tunisia.